Title
Progress in measurements and modeling of fast-ion Dα light

Journal
39th EPS Conference on Plasma Physics 2012, EPS 2012 and the 16th International Congress on Plasma Physics, 2

ISBN
9781622769810

Authors
Heidbrink, WW
Bortolon, A
Grierson, BA
et al.

Publication Date
2012-12-01

Progress in Measurements and Modeling of Fast-ion D_α Light

W.W. Heidbrink[1], A. Bortolon[1], B.A. Grierson[2], D. Liu[1], G.R. McKee[3], C.M. Muscatello[4], M. Podestà[2], and E. Ruskov[1]

[1]*University of California, Irvine, California, USA*
[2]*Princeton Plasma Physics Laboratory, Princeton, New Jersey, USA*
[3]*University of Wisconsin, Madison, Wisconsin, USA*
[4]*University of California, Davis, California, USA*

The fast-ion D_α (FIDA) diagnostic technique exploits the Doppler shift of the Balmer-alpha emission from neutralized deuterons to obtain velocity and profile information about the fast-ion distribution function. An overview of "active" FIDA measurements (using a diagnostic beam) appears in [1]. This paper summarizes recent efforts to understand and validate FIDA measurements on the DIII-D and NSTX tokamaks.

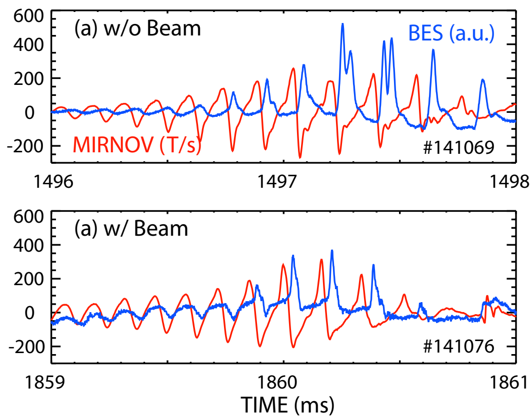

Figure 1: Mirnov coil and ac-coupled "BES" signals during off-axis fishbone bursts in discharges (a) without and (b) with an active beam in the "BES" sightline. The passive FIDA light is brighter than the dc beam emission (which is ~80 units on this scale).

A recent paper [2] shows that "passive" FIDA light (from reactions with edge neutrals) can also be important. Standard "BES" diagnostics use a bandpass filter to measure Doppler-shifted beam emission from an injected beam. Although beam emission is normally 1-2 orders of magnitude brighter than FIDA emission, passive FIDA light can be brighter than beam emission when instabilities deposit large quantities of fast ions in the scrapeoff region. Figure 1 shows an example during off-axis fishbone [3] activity in DIII-D. Two bursts of similar strength that cause ~8% drops in neutron rate are shown. In one case, the active beam in the "BES" sightline is off while, in the other case, the active beam is on, so no beam emission is present in the first case. Nevertheless, the measured signals are very similar in amplitude, indicating that fluctuations in passive FIDA light exceed fluctuations in beam emission for these conditions. The phenomenon is similar to the large bursts of passive signal seen on neutral particle analyzer (NPA) diagnostics when instabilities expel fast ions to the edge. It occurs because the edge neutral density is generally orders of magnitude larger than the injected neutral density. The observed signals from instabilities and from prompt losses are consistent with rough estimates of the expected intensity. Measurement of passive FIDA light could be the basis for a novel dedicated fast-ion loss diagnostic.

For active FIDA measurements, the DIII-D facility is equipped with FIDA imaging [4] and three spectroscopic diagnostics with vertical, oblique and tangential views of the plasma. The vertically-viewing profile diagnostic employs a Czerny-Turner spectrometer tuned to the blue side of the cold D_α line. The instrument has ~ 0.3 nm spectral resolution, typical temporal resolution of 5 ms, and collects a ~ 1 cm light cone at beam intersection. The obliquely-viewing diagnostic [5] employs a transmission grating spectrometer that only measures the blue-shifted side of the spectrum. A bandpass filter transmits the blue wing but strongly attenuates the cold D_α line. The instrument has spectral resolution of ~ 0.5 nm, temporal resolution of 1 ms, and collects a ~ 5 cm light cone at beam intersection. The main-ion charge exchange recombination (CER) diagnostic [6] measures the entire D_α feature with a pair of tangential views. It employs a Czerny-Turner spectrometer and a 12-bit CCD camera. For FIDA measurements, the pixels at the cold D_α line are allowed to saturate weakly. Typical temporal resolution is 5 ms and the analysis procedure fits the entire spectrum [6]. Although the oblique instrument includes reference views, all three diagnostics normally use beam modulation to remove the background. Recent work confirms the value of multiple views. Comparison of data from the different instruments shows that the sawtooth instability causes greater transport of passing fast ions than of trapped ones [7]. In a comparison of different angles of beam injection, the more tangential sources produce larger signals on the tangential and oblique diagnostics, while the more perpendicular sources produce larger signals on the vertical diagnostic [8].

The FIDASIM code models active FIDA and NPA signals, as well as beam, direct charge-exchange, halo, and visible bremsstrahlung (VB) emission. The physics assumptions of the code are described in Ref. [9]. Recently, three "bugs" were identified that effect results published in two publications [6, 8]. The most important of these resulted in an overestimate of the lifetime of halo neutrals, which increased the predicted halo and FIDA emission. Another "bug" involving incorrect cross sections produced a $\sim$10% overestimate of FIDA light. A third "bug" caused distortions in the predicted spatial profile. These errors as well as an adjustment of the DIII-D injection geometry are corrected in the version employed in this paper (FIDASIM 4.0).

One general conclusion from recent studies is that it is highly desirable to measure multiple features of the D_α spectrum [10]. The tangentially viewing main-ion CER diagnostic measures the entire spectrum and compares all of the spectral features with FIDASIM [6]. Good agreement of the beam emission with the prediction provides confidence in the modeling of the injected neutral population and the atomic physics in the code. Good agreement between the predicted and measured VB confirms the validity of the intensity calibration. However, for this diagnostic, when using FIDASIM 4.0, the code underpredicts both the thermal and FIDA emission, suggesting that the halo density is underestimated.

Discharges with modest beam power and negligible MHD are usually chosen for these diagnostic tests. Figure 2 shows results from a FIDA calibration discharge of this type. At large Doppler shift, the net signal is approximately zero, as it should be if the background subtraction is accurate. However,

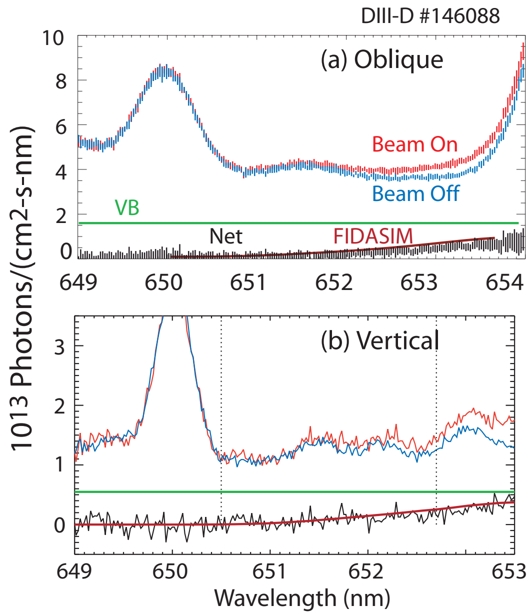

Figure 2: Spectra for channels from the (a) oblique and (b) vertical diagnostics in an MHD-quiescent discharge with injection of one steady 65 keV beam and 10 ms blips of the diagnostic active beams every 200 ms. The "net" signal between the "beam-on" and "beam-off" spectra is the blue-shifted FIDA feature, which is in excellent agreement with the FIDASIM prediction for this case. The predicted VB level is also shown. (The cold D_α line is at 656.1 nm.)

the observed baseline at large Doppler shift is twice as large as the predicted VB. This discrepancy is attributed to scattered light. Both the spectral shape and the magnitude of the FIDA feature are in excellent agreement with the prediction.

A new capability at DIII-D is vertical steering of one of the beamlines so that two sources inject off-axis. In a number of discharges designed to test this new capability, each of the available sources injected for ∼100 ms, followed by a 10 ms blip of the FIDA active beams [8]. Figure 3 shows one of these comparisons. The FIDA data show that the central fast-ion density is much lower with off-axis injection than with on-axis injection. All available diagnostics confirm this result. Quantitatively, it was found that the vertically-tilted sources produce ∼20% fewer fast ions than expected, probably due to an error in the reported beam power. This study also provided a good test of the active NPA signals produced by trapped fast ions near the magnetic axis. Comparison with FIDASIM predictions shows good agreement between theory and the NPA data.

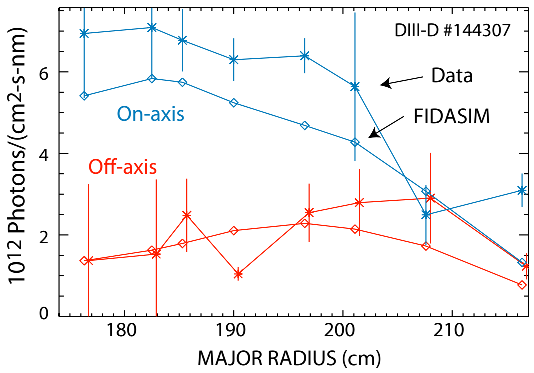

Figure 3: Vertical FIDA profiles during (blue) on-axis injection of a single near-perpendicular source and during (red) off-axis injection of a single near-tangential source. The data (*) agree well with theory (⋄). Spectral integration from 650.5-652.7 nm.

Dedicated FIDA experiments have been conducted at NSTX with the vertically-viewing s-FIDA diagnostic [11]. This instrument uses a transmission grating spectrometer in conjunction with a CCD camera to measure D_α spectra between 645-667 nm. An OD2 neutral density filter in the spectrometer image plane partially blocks the cold D_α center line. The spectral resolution is ∼ 0.23 nm and the data are acquired in 10 ms time bins. To minimize MHD activity, a single modulated (50 Hz at 50% duty cycle) 65 keV neutral beam is injected into plasmas with different values of plasma current I_p, density n_e, and toroidal field B_T. For vertical views in a conventional tokamak, the blue- and red-shifted sides of the spectrum should be nearly identical but, in a spherical tokamak, owing to the large field-line pitch and fast-ion gyroradius, large asymmetries are expected. Of the beam-driven instabilities that are commonly observed in NSTX, low-frequency instabilities such as the toroidal Alfvén eigenmode (AE) were absent but, despite the low beam power, MHz global or compressional AEs were present in these discharges. The measured neutron rate agrees well with TRANSP predictions during the low-power phase, suggesting that any spatial transport caused by the MHz instabilities is modest. Raw data from this experiment appear in Ref. [10]. Comparison between the measured and calculated VB baselines shows that the measured value is about half of the predicted value, implying that the experimental calibration is erroneously low. There are also difficulties with the background subtraction for some of the data. For some channels, offsets are observed at Doppler shifts above the injection energy; also, the net signal from beam modulation sometimes disagrees with the net signal derived from the reference views. Operating at low beam power to minimize MHD aggravates the difficulties in background subtraction. Analysis shows that scattered light is responsible for the baseline offsets.

Despite these experimental difficulties, the NSTX diagnostic unquestionably measures FIDA light. The spectral shape is in excellent agreement with theory [Fig. 4(a)]. Apart from the extreme channels on the red-shifted side of the spectrum (where the difficulties with background subtraction are largest), the spatial profiles agree reasonably well with theory (Fig. 4). Figure 5 compares the scaling of the spatial profile with theory for all of the discharges in the dedicated experiment. As predicted, the location of the peak of the red-shifted profile occurs at larger major radius than the peak of the blue-shifted profile [Fig. 5(a)]. Despite considerable scatter, the observed variations in position also correlate with theory (correlation coefficient $r \simeq 0.5$ for both sides of the spectrum). The correlation between the measured and predicted brightness is excellent ($r > 0.9$ for both sides of the spectrum). As expected, the blue-shifted side is brighter than the red-shifted side.

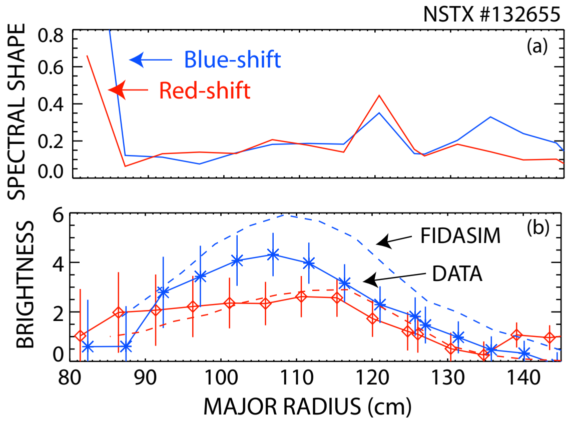

Figure 4: (a) Reduced χ^2 for a comparison between the measured FIDA spectrum and the spectral shape predicted by FIDASIM vs major radius. Both sides of the spectrum agree well with theory. (b) Measured (symbols) and predicted (dashed) spatial profiles for the red- and blue-shifted sides of the spectrum. The data and theory are averaged over 140 ms and the theory is divided by a factor of 7.

The support of the DIII-D and NSTX teams is gratefully acknowledged. This work was funded by the US Department of Energy under SC-G903402, DE-FC02-04ER54698, DE-FG03-02ER54681, and DE-FG02-06ER54867.

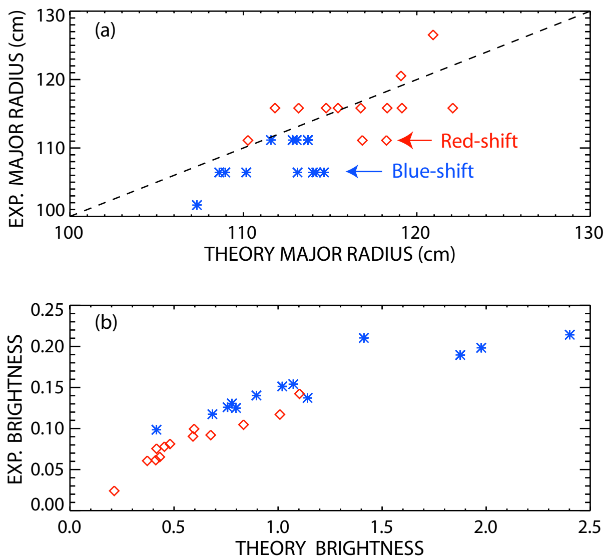

Figure 5: (a) Measured position of the peak of the spatial profile vs FIDASIM prediction for the blue-shifted (*) and red-shifted (⋄) sides of the spectrum for the 13 discharges in the dedicated NSTX experiment. The line indicates agreement between theory and experiment. (b) Measured experimental brightness vs FIDASIM prediction. The brightness is the sum of the signals for the five spatial channels closest to the peak.

References

[1] W.W. Heidbrink, Rev. Sci. Instrum. **81** (2010) 10D727.
[2] W.W. Heidbrink, *et al.*, Plasma Phys. Controlled Fusion **53** (2011) 085007.
[3] M. Okabayashi, *et al.*, Phys. Plasma **18** (2011) 056112.
[4] M.A. Van Zeeland, *et al.*, Plasma Phys. Controlled Fusion **51** (2009) 055001.
[5] C.M. Muscatello *et al.*, Rev. Sci. Instrum. **81** (2010) 10D316.
[6] B.A. Grierson, *et al.*, Phys. Plasma **19** (2012) 056107.
[7] C.M. Muscatello, *et al.*, Plasma Phys. Controlled Fusion **54** (2012) 025006.
[8] W.W. Heidbrink, *et al.*, Nucl. Fusion **52** (2012) in press.
[9] W.W. Heidbrink, *et al.*, Comm. Comp. Physics **10** (2011) 716.
[10] W.W. Heidbrink, *et al.*, Rev. Sci. Instrum. **83** (2012) submitted.
[11] M. Podestà, *et al.*, Rev. Sci. Instrum. **79** (2008) 10E521.